Non-destructive testing on a stone masonry using acoustic attenuation tomography imaging

G. Concu[1], B. De Nicolo[1], C. Piga[2], V. Popescu[3]
[1]Department of Structural Engineering,
University of Cagliari, Italy
[2] Department of Land Engineering,
University of Cagliari, Italy
[3]Department of Electronics,
University of Transilvania, Romania

Keywords: non destructive testing, computerised tomography, acoustic attenuation, spectral frequency centroid downshift, stone masonry.

The present paper illustrates the preliminary results of an experimental program started with the aim of pointing out the reliability of computerized attenuation tomography imaging in the diagnosis and characterization of building structures.

The computerized acoustic tomography is an emerging technique for advanced imaging of materials. The spatial distribution of acoustic velocity and attenuation are imaged and then correlated with properties directly related to physical conditions. The velocity is determined by the elastic properties and density, while the attenuation is determined by the inelastic property of the medium. Experimental has demonstrated that attenuation is more suitable than velocity to study the internal properties of materials, because an anomaly has a greater effect on the attenuation of a signal than on the propagation time. In fact, wave's characteristics such as attenuation, scattering and frequency content may allow one to get relevant information about the material, because of the reliance of the propagation on the properties of the medium through which waves travel. Different materials absorb or attenuate the wave power at different rates, and waves are reflected by boundaries between dissimilar materials, so that changes in materials structure, e.g. presence of discontinuities or defects, can affect amplitude, direction, and frequency content of scattered signals. Following this trend, this study has been focused on the attenuation tomography.

The attenuation tomography has been carried out on a full scale real stone masonry affected by a defect consisting in a macro-cavity. In detail, the tomographic analysis has been performed on a horizontal plane section crossing the wall in order to intercept the void. Due to the uncertainties of measurements, a set of redundant measures has been acquired, so that an over determined equations system has been solved. According to a model developed by Quan and Harris [1], a signal attenuation coefficient α_0 has been defined, and a statistically based method that estimates the

attenuation coefficient from the spectral centroid downshift over a range of frequencies has been performed. The model states that the spectral centroid downshift is proportional to a path integral through the attenuation distribution and can be used as observed data to reconstruct the attenuation distribution tomographically. The tomographic problem has been implemented in Matlab® software environment. Numerical modelling assumes straight rays from source transducer to receivers, and involves an ill conditioned system of linear equations. The SIRT (Simultaneous Iteration Reconstruction Technique) iterative method has been implemented and applied to solve the system. The solving algorithm has been implemented in an automated procedure that allows the user to easily obtain a map of the attenuation distribution in the tomographic section. The LabView®'s native virtual instruments have been used.

The preliminary results since now achieved showed that the computerized attenuation tomography imaging can successfully apply to the stone masonry, and confirmed the suitability of the proposed approach to non destructive testing of building materials.

References

[1] Y. Quan, J.M. Harris, “Seismic attenuation tomography using the frequency shift method”, Geophysics, 62(3), 895-905, 1997.

Abstract

In this paper, the computerised acoustic attenuation tomography imaging has been analysed, implemented and then performed for non destructive testing of a stone masonry. The tomography implies that a ill posed linear equations system has to be solved, in order to determine the attenuation distribution inside the tested structure, thus highlighting the presence of anomalies. The algebraic problem of the attenuation tomography inversion has been deepened, and the solving algorithm has been numerically developed. The entire process has been implemented in an automated procedure that allows the user to easily obtain a map of the attenuation distribution in the tomographic section of the object.

Keywords: non destructive testing, computerised tomography, acoustic attenuation, spectral frequency centroid downshift, stone masonry.

1 Introduction

Inspection and monitoring of structural conditions is an essential part of civil engineering systems' life-cycle management. In the last decades, extending the useful service life of structures and infrastructures has become of crucial importance, due to cultural, social, and economic factors. Management and maintenance systems for assets and structures have been developed in order to handle the information flow and store relevant data, to plan and organise the maintenance activities, and to prepare and manage maintenance budgets. In the field of assessment methodologies particular importance is given to developments of Non-Destructive Techniques (NDTs), including automated procedures and information technology to support decision making and evaluation of data. NDTs are particularly suitable when dealing with structures and infrastructures because they allow one to not interfere with the state of the asset [1]. As a major NDT tool, acoustic techniques, based on measurements of the characteristics of acoustic waves

propagating through the material, are often used in quality control and quality assessment for engineering projects for structures and infrastructures [2-5]. The studies of acoustic techniques have been focused on medical or materials engineering applications for laboratory testing. The valuable handmade analysis has begun in the first of '90 [6-11] and nowadays it is performed using considerable approximations to the detriment of results precision. The inaccurate results are also caused by the subjective methodology often used for interpretations. This contributed to form the common opinion that the use of such methodologies to analyze buildings does not give reliable results. Conversely, the aforesaid techniques could show notable diagnostic properties if used in an appropriate way, that is providing them with innovative techniques, which employ and develop advanced computational tools and testing devices. In the light of this, fuelled by the rapid development of portable personal computers, high-performance computing algorithms and electronic engineering technology, acoustic techniques have evolved dramatically during recent years [12-16].

Following this trend, an experimental program has been started, with the aim of pointing out the reliability of the computerised acoustic attenuation tomography, an emerging technique for advanced imaging of materials, in the diagnosis and characterization of building structures.

The algebraic problem of the attenuation tomography inversion has been deepened, and the solving algorithm has been numerically developed. The solving algorithm has been implemented in an automated procedure that allows the user to easily obtain a map of the attenuation distribution in the tomographic section of the object. The procedure has been since now performed on a full scale real masonry affected by a defect consisting in a macro-cavity sets in central position, and the present work reports the preliminary results of this application.

2 Generalities on acoustic methods

Among the various NDTs, acoustic ones appear to be of great usefulness since they are non-invasive, easy to use and of a general rather than specific nature, thus they are often used in structural diagnosis. They are utilised directly in the field for investigations of a wide range of structures and infrastructures, and in laboratory for materials characterisation.

Acoustic material analysis is based on a simple principle of physics: the propagation of any wave will be affected by the medium through which it travels. Thus, changes in measurable parameters associated with the passage of a wave through a material can be correlated with changes in physical properties of the material.

Traditional application of acoustic techniques is based on measurements of the velocity v of acoustic waves propagating through the material. The velocity is obtained from the ratio l/t, where t (travel time) is the time wave needs to travel along the path of length l. The wave velocity is directly related to structure's elastic parameters, e.g. elastic modulus E, Poisson's number ν and density ρ, thus its analysis provides information crucial for inspections of structures' stability and lastingness.

Nevertheless, other wave's characteristics such as attenuation, scattering and frequency content, primarily related to the elastic wave power, may allow one to get more and relevant information about the material. In fact, wave power is absorbed or attenuated at different rates in different materials, determined in a complex manner by interactive effects of density, hardness, viscosity, and structure. Moreover, waves reflect from boundaries between dissimilar materials, thus changes in material structure, e.g. presence of discontinuities or defects, can affect the amplitude, direction, and frequency content of scattered signals. Finally, all materials tend to act to some degree as a low pass filter, attenuating or scattering the higher frequency components of a broadband wave more than the lower frequency components. Thus, analysis of changes in the remaining frequency content of a selected broadband pulse that has passed through the test material can keep track of the combined effects of attenuation and scattering as previously described [17-19].

Acoustic techniques are preferentially carried out applying the Direct Transmission Technique, in which the wave is transmitted by a transducer (Emitter) through the tested object and received by a second transducer (Receiver) on the opposite side. This testing modality allows to acquire the signal after it has travelled through the object's thickness, from the emitter to the receiver. For instance, the Direct Transmission Technique permits to measure the time t that the wave needs to travel through the object's thickness, from the emitter to the receiver, along a path of length l; the average velocity of the wave is then obtained from the ratio l/t [20]. The Direct Transmission Technique is very effective, since the broad direction of wave propagation is perpendicular to the source surface and the signal travels through the entire thickness of the item. Standards concerning the determination of waves velocity in structures, e.g. Europeans EN 12504-4 [21] and EN 14579 [22], suggest, therefore, the application of this kind of signals transmission.

The Direct Transmission Technique has some limits too. The major limit consists in describing the wave's characteristics field of the object using for each path only one value of that characteristic, i.e., hypothesising that the mean value is homogeneous along each wave path. This assumption prevents from pinpointing the position of the detected anomaly inside the object. A promising way for overcoming this limit is the use of the tomographic technique, which uses numerical analysis as a real measurement instrument, combining the results of several Direct Transmission Technique applications for a sharper and reliable investigation of the object [23-26].

3 Computerized Acoustic Tomography

One emerging technique for advanced imaging of materials is Computerised Acoustic Tomography. The Computerised Acoustic Tomography uses technology invented for the biomedical field [27] to display the interior of engineered structures. The spatial distribution of acoustic velocity and attenuation are imaged and then correlated with properties directly related to physical conditions [28-34]. The velocity is determined by the elastic properties and density, while the attenuation is determined by the inelastic property of the medium.

It has long been believed that attenuation is more suitable than velocity (or travel time) to study the internal properties of materials, because an anomaly has a greater effect on the attenuation of a signal than on the propagation time [35, 36]. In fact, as previously mentioned, wave's characteristics such as attenuation, scattering and frequency content may allow one to get relevant information about the material, because of the reliance of the propagation on the properties of the medium through which waves travel. Different materials absorb or attenuate the wave power at different rates, depending on complex interactive effects of material characteristics, such as density, viscosity, homogeneity. Additionally, waves are reflected by boundaries between dissimilar materials, so that changes in materials structure, e.g. presence of discontinuities or defects, can affect amplitude, direction, and frequency content of scattered signals.

3.1 Travel Time Tomography

An acoustic wave propagating through any object spends a definite time to travel from a point to another of the object. The wave covers the path between the two points spending the time t and propagating with a mean velocity v. When the distance between the two points reduces to zero a local velocity v_p, and a local slowness $s = 1/v_p$ can be defined for the point p.
The equation for travel time can be written as:

$$\int_{ray} 1/v \, dl = \int_{ray} s \, dl = t \qquad (1)$$

The acoustic behaviour of a selected section of the object is then defined when the slowness s is known continuously in every point of the investigated section. This function can be approximated dividing the section into a grid of N rectangular cells (pixels) in which v is supposed to be constant.

The tomographic problem consists in obtaining the slowness of the N pixels starting from the knowledge of M travel times measured along a series of paths joining couples of transducers located on opposite or adjacent sides of the section (Figure 1).

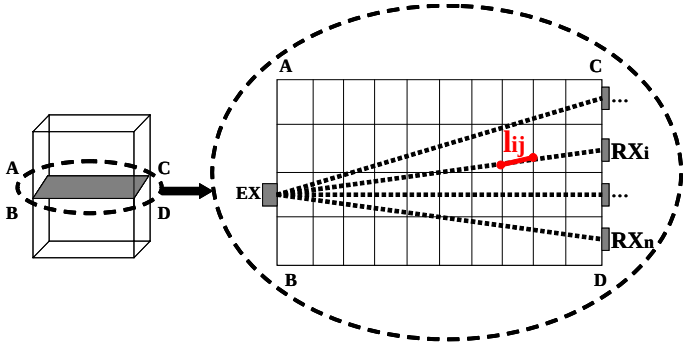

Figure 1: Schema of linear tomographic problem.

The ray-paths of waves depend on the velocity distribution, and their sharp definition is a not easy problem to solve, especially when dealing with structures made of different elements such as stone masonry. A valid approximation may be the Linear Tomography, which considers the ray-paths to be rectilinear.

In order to obtain the values of the slowness in the grid, the following equations system, which is the matrix form for equation (1), has to be solved:

$$Ls = t \tag{2}$$

where :

$t = [t_1, t_2, \ldots t_M]$ is the vector of measured travel times;

$s = [s_1, s_2, \ldots s_N]$ is the vector of slowness;

$L = [l_{11}, l_{12}, \ldots l_{NM}]$ is the coefficients matrix, whose generic element l_{ij} is the length of the i^{th} ray in the j^{th} cell.

Thus, the tomographic solution consists in determining the vector s as:

$$s = L^{-1} t \tag{3}$$

To avoid instability in matrix inversion, the number of cells must be smaller than the number of measured travel times. If the inverse of L exists it can be directly evaluated. However, the inverse of L generally does not exist since L is not a square matrix, it is ill conditioned, and it has not full rank. Thus, other methods, such as iterative ones, have to be used to solve the problem.

3.2 Attenuation Tomography

For the purpose of estimating attenuation, the process of waves propagation can be assumed as described by linear system theory. If the amplitude spectrum of an incident wave is $S(f)$ and the instrument/medium response is $G(f) \cdot H(f)$, then the received amplitude spectrum $R(f)$ may be, in general, expressed as :

$$R(f) = G(f) \cdot H(f) \cdot S(f) \tag{4}$$

where the factor $G(f)$ includes geometrical spreading, instrument response, source/receiver coupling, radiation patterns, and reflection/transmission coefficients, and the phase accumulation caused by propagation, and $H(f)$ describes the attenuation effect on the amplitude. It can be assumed that the effects included in factor $G(f)$ are not frequency dependent. Thus, it can be simplified as $G(f) = G$.

For the purpose of this study, the $H(f)$ factor is of greater interest. Experiments indicate that attenuation is usually proportional to frequency [37], that is, response $H(f)$ may be expressed as:

$$H(f) = exp\ (-f \cdot \int_{ray} \alpha_0\ dl) \tag{5}$$

where the integral is taken along the ray-path, and α_0 can be regarded as an intrinsic attenuation coefficient. The tomography's goal is to estimate the medium response

H(f), or more specifically, the attenuation coefficient α_0, from knowledge of the input spectrum *S(f)* and the output spectrum *R(f)*.

A direct approach is to solve equation (5) by taking the logarithm and obtaining:

$$\int_{ray} \alpha_0 \, dl = 1/f \cdot \ln [G \cdot S(f) / R(f)] \tag{6}$$

Equation (6) may be used to estimate the integrated attenuation at each frequency and is called the amplitude decay method. However, as described above, the factor *G* lumps many complicated processes together, and is very difficult to be determined. Furthermore, the calculation of attenuation based on individual frequencies is not robust because of poor individual signal-to-noise.

To overcome these difficulties, Quan and Harris [38] developed a statistically based method that estimates the attenuation coefficient α_0 from the spectral centroid downshift over a range of frequencies.

The centroid frequency of the input signal *S(f)* is defined as:

$$f_S = \frac{\int_0^\infty f S(f) df}{\int_0^\infty S(f) df} \tag{7}$$

and the variance is:

$$\sigma_S^2 = \frac{\int_0^\infty (f - f_S)^2 S(f) df}{\int_0^\infty S(f) df} \tag{8}$$

Similarly, the centroid frequency of the received signal *R(f)* is:

$$f_R = \frac{\int_0^\infty f R(f) df}{\int_0^\infty R(f) df} \tag{9}$$

and its variance is:

$$\sigma_R^2 = \frac{\int_0^\infty (f - f_R)^2 R(f) df}{\int_0^\infty R(f) df} \tag{10}$$

where *R(f)* is given by equation (4). If the factor *G* is independent on frequency *f*, then f_R and σ_R^2 will be independent on *G*. This is a major advantage of using the spectral centroid and variance rather than the actual amplitudes.

For the special case where the incident spectrum *S(f)* is Gaussian, under the assumption of a linear-dependence model of attenuation to frequency, the attenuation coefficient α_0 can be estimated by assuming that:

$$\int_{ray} \alpha_0 \, dl = (f_S - f_R) / \sigma_S^2 \tag{11}$$

where f_S and f_R are the centroid frequency for the source and receiver, respectively, and σ_S is the variance, or bandwidth, of the source signal. The previous relationship states that the attenuation is proportional to the centroid frequency difference which

has downshifted from the original source centroid f_S, to the centroid of the received signal f_R. The total amount of centroid frequency downshift depends on the attenuation characteristics along the acoustic ray-path.

The tomographic formula relating frequency shift with the attenuation projection is exact only for Gaussian spectra, i.e., equation (11). Nevertheless, similar derivations can also be obtained for other frequency compositions, which implies that the estimates of relative attenuation are not sensitive to small changes in spectrum shapes, and points out the robustness of this method.

Equation (11) is in the same form as (1), with the intrinsic attenuation coefficient α_0 in (11) corresponding to the slowness $1/v$ in (1). The expression of frequency centroid difference in (11) corresponds to the travel time t in (1). This similarity makes the attenuation tomographic inversion easy to conduct applying the iterative algorithms developed for travel time tomography, simply replacing $1/v$ with α_0 and t with $(f_S - f_R)/\sigma_S^2$.

As stated above, equation (11) is the basic formula for attenuation tomography. It can be written also in a discrete form as:

$$\sum_{j=1}^{N} l_{ij}\,\alpha_{0j} = \frac{f_{Si} - f_{Ri}}{\sigma_{Si}^2} \qquad (i = 1,..M) \tag{12}$$

where i represents the i^{th} ray, j the j^{th} parameterized cell of the medium, and l_{ij} is the length of the i^{th} ray in the j^{th} cell (Figure 2).

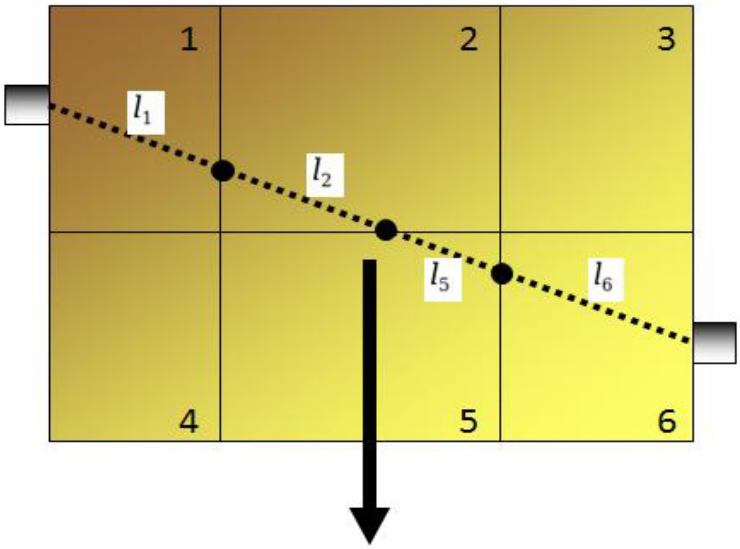

$$\int_{i^{th}\ ray} \alpha_0\, dl = a_{01}l_1 + a_{02}l_2 + a_{05}l_5 + a_{06}l_6 = (f_{Si} - f_{Ri})/\ \sigma_{Si}^2$$

Figure 2: Example of tomography system equation.

The previous equations system can be written in matrix form as:

$$L\,a = F \tag{13}$$

where :
$F = [F_1, F_2, \ldots F_M]$ is the vector of calculated centroid frequency downshift, in which $F_i = (f_{Si} - f_{Ri}) / \sigma_{Si}^2$ has been assumed;
$a = [\alpha_{01}, \alpha_{02}, \ldots \alpha_{0N}]$ is the vector of attenuation coefficients;
$L = [l_{11}, l_{12}, \ldots l_{NM}]$ is the coefficients matrix, whose generic element l_{ij} is the length of the i^{th} ray in the j^{th} cell.

The intrinsic attenuation coefficient α_0 is in the unit of decibel second per metre ($dBsm^{-1}$).

4 Experimental

The attenuation tomography analysis has been carried out on a full scale real stone masonry. The wall is 90 cm wide, 62 cm high and 38 cm thick, and it is made of Trachite blocks sized 20 × 38 × 12 cm^3, settled as shown in Figures 3 and jointed with cement lime mortar. The block assigned to the central position of the wall was not settled, thus realising a macro-cavity with the same size of the missing block, and assumed as a known anomaly. Mortar joints have been assumed to be 1cm thick, but since the wall was manually built by a builder, actual dimensions are not so precise.

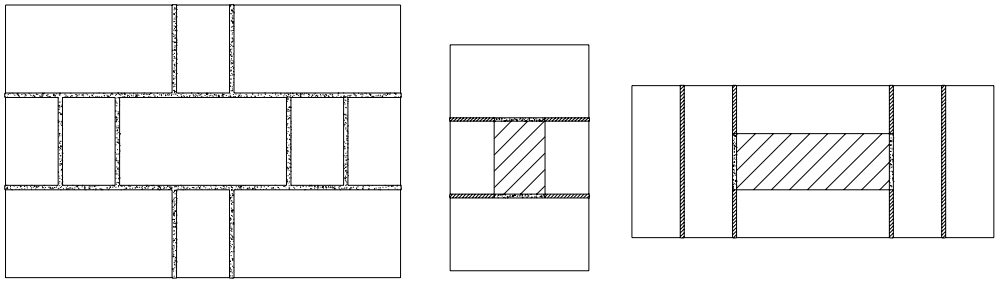

Figure 3: The full scale real masonry. From left to right: front view, vertical section, horizontal tomographic section.

The acoustic wave is transmitted through the test object and received by a second transducer positioned in one of the faces of the structure. Changes in received signal provide indications of variations in material continuity.

4.1 The Tomographic Analysis

The attenuation tomography has been applied to a horizontal plane section crossing the wall in order to intercept the central void (Figure 3). The investigated section was 90 cm wide and 38 cm thick, and it has been divided in 40 cells 9 cm × 9.5 cm.

Emitters and receivers have been alternatively positioned along the side of the section, in the centres of the cells. Each acquisition has been run activating the receivers positioned in the sides of the wall parallel and adjacent to the side where the emitter was positioned (Figure 4).

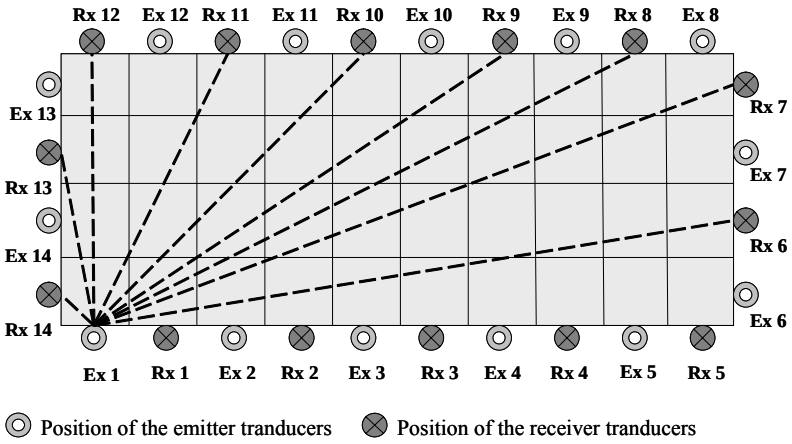

Figure 4: Measurements schema.

Using this measurements configuration, the section is crossed by 138 paths, and the section coverage is excellent. For each ray-path the quantity $(f_S - f_R)/\sigma_S^2$ has been calculated. Thus, system (13) consists in 138 equations and 40 unknowns.

4.1.1 Resolution of the tomographic problem

Because of the non-linear relationship between the attenuation coefficient and the centroid frequency downshift, it is almost impossible to find the solution by a single step algorithm using a linear approximation. Thus, iterative methods [39, 40] can be used, such as ART (Algebraic Reconstruction Technique) [41, 42] and SIRT (Simultaneous Iteration Reconstruction Technique) [43-45]. Both methods need a starting value of attenuation, and then they modify iteratively this value by minimising the difference between the measured centroid frequency downshift and the centroid frequency downshift calculated in the previous iteration. While ART goes on ray-path after ray-path, SIRT takes into account the effect of all ray-paths crossing each cell.

In the N-dimensional space each equation in (13) represents a hyperplane. When a unique solution exists, the intersection of all the hyperplanes is a single point. A computational procedure to locate the solution consists in starting with an initial solution, denoted by:

$$a^{(0)} = \left(a_1^{(0)}, a_2^{(0)}, \ldots, a_N^{(0)}\right) \tag{14}$$

This initial solution is projected on the hyperplane represented by the first equation in (13) giving $a^{(1)}$. $a^{(1)}$ is then projected on the hyperplane represented by the second equation in (13) to yield $a^{(i-1)}$ and so on. When $a^{(i-1)}$ is projected on the hyperplane represented by the i^{th} equation to yield $a^{(i)}$, the process can be mathematically described by:

$$a^{(i)} = a^{(i-1)} + \frac{b_i - \vec{l}_i^T a^{(i-1)}}{\vec{l}_i^T \vec{l}_i} \vec{l}_i \tag{15}$$

where l_i is the i^{th} raw of the matrix L.

For an over determined problem, $M > N$, ART does not give a unique solution, but this depends on the starting point. The tomographic system is often over determined and measurement noise is present. In this case a unique solution does not exist and the solution found by ART will oscillate in the neighbourhood of the intersections of the hyperplanes. The SIRT algorithm uses the same equations as in the ART algorithm; the difference is that SIRT modifies the attenuation model taking into account at each iteration the effect of all ray-paths crossing each cell. The new value of each cell is the average value of all the computed values for each hyperplane. Then, using the SIRT algorithm, better solutions are usually obtained at the expense of slower convergence.

In this study the tomographic problem has been implemented in Matlab® software environment. Numerical modeling assumes straight rays from source transducer to receivers, and involves an ill conditioned system of linear equations. The SIRT method has been applied to solve the system.

4.1.2 The instrumental set

The testing equipment has been developed and assembled specifically for revealing the advantages of the tomography method applied to destructive testing of building materials and structures. It includes:

- 1 wide band piezoelectric transducer GRW350-D50 produced by Ultran for emitting signals. The transducer has a diameter of 520mm and a central frequency of 370 kHz. It is fed with a high-voltage input signal (200 V) necessary to overcome the increased impedance of the construction materials in this range of frequencies;
- 8 receiving sensors VS150-M manufactured by Vallen Systeme for receiving signals. The transducers have very good wide band frequency response in the band of interest (150 - 500 kHz), and coupled with their own preamplifiers offer enough sensitivity to perform the required measurements. The sensors are disposed linearly on a plastic rod and are receiving at the same time the signal transmitted by the emitting transducer;
- a signal generator Tektronix AFG3011, whose output was further amplified;
- an oscilloscope Tektronix DPO3014;
- a National Instruments PXI Data Acquisition System with two PXIe-6124 boards. The output of the sensors, preamplified, is fed into this acquisition system where it is digitally converted with a resolution of 16 bits per sample;
- a PC for data storage and signal processing.

The software for controlling the acquisition system has been built in LabView® environment.

Because of the huge importance of signal/noise ratio for FFT spectral analysis, a broadband sweep signal has been used as source signal. This signal shows a linear relationship between time and frequency. The purpose of this choice was to extend the frequencies involved in measurements to a range up to 300 KHz, with the aim of increasing the analysis resolution and of estimating the attenuation coefficient more

accurately in a wide band of signal. Indeed, the evaluation of the attenuation coefficient requires a spread spectrum of both transmitted and received frequencies in order to estimate centroid frequency and variance values.

4.1.3 The automated procedure

Using LabView®, an automation of the entire measuring process has been designed, recording the received signals, eight per measurement, in various points of the structure under test. Taking into consideration the position of the transmitter and the receivers, and the received signals as a function of the transmitted ones, a map of the attenuation distribution in the tested section of the structure has been drown.

LabView®'s native virtual instruments have been used for implementing the controls for the data acquisition system. The automation specific software, implemented with the Rapid Application Development (RAD) environment WinDev®, has been interfaced with the LabView® virtual instruments using ActiveX controls and text files for passing the acquired data. The entire software system has been packed under a user-friendly interface which allows the user to follow a step-by-step procedure in order to get the measurements results under the form of a graphic tomographic map.

4.2 Results

The result of the implemented algorithm is a distribution map of the attenuation coefficient in the selected section of the investigated sample. This map is shown in Figure 5.

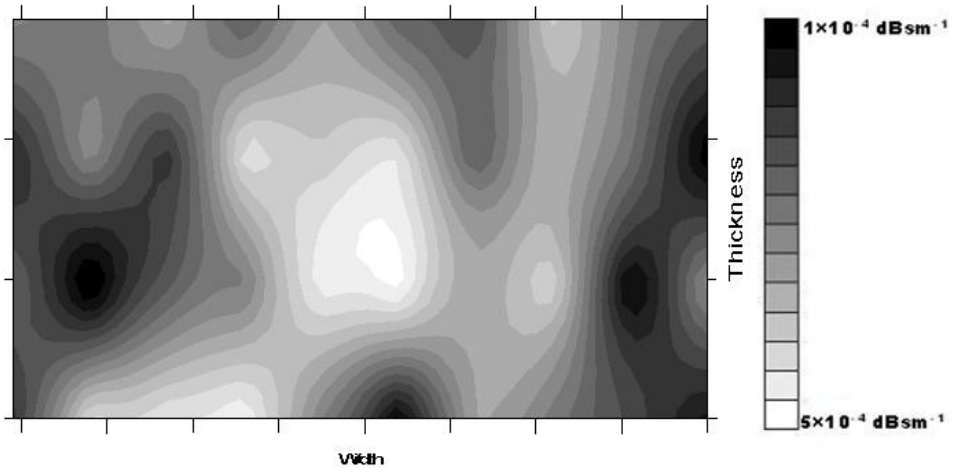

Figure 5: Distribution of the attenuation coefficient in the tomographic section.

The map of the attenuation coefficient is represented by a 256 levels grey scale diagram, where the lowest level (white) corresponds to the maximum attenuation coefficient, and the highest level (black) corresponds to the minimum attenuation coefficient. The 256 levels are normalised with respect to the range of attenuation

coefficients measured in the represented tomography. The 10×4 cells are represented by using the Kriging method [46, 47].

The SIRT algorithm has been tested for 1000 iterations starting from different initial points, i.e., a vector of zeros and the vector composed by the average attenuation coefficient of the ray paths crossing each cell. The algorithm found the minimum after 100 iterations. The calculation time has been of 0.9 s.

As it can be seen, the SIRT results represented by the Kriging method identify a central region, corresponding to the position of the cavity, where the attenuation coefficient of the wave is higher. However, the contours of the cavity area are not well defined, and the attenuation distribution is quite scattered. On the one hand this result points out that the attenuation coefficient has a very high sensitiveness to all kind of material discontinuity which causes energy loss, e.g. mortar joints and mortar intrusions, different elastic and physic properties of stones, thus it is valid for the surveying purpose; on the other and it is worth noting that using more thick grids for data acquisition and testing some other inversion methods could make possible to define with better precision the shape of the defects, thus achieving a sharper resolution.

5 Conclusion

The present paper illustrates the preliminary results of an experimental program started with the aim of pointing out the reliability of computerised attenuation tomography imaging in the diagnosis and characterisation of building structures. The attenuation tomography has been carried out on a full scale real stone masonry affected by a defect consisting in a macro-cavity sets in central position. In detail, the tomographic analysis has been performed on a horizontal plane section crossing the wall in order to intercept the central void. Due to the uncertainties of measurements, a set of redundant measures has been acquired, so that an over determined equations system has been solved.

According to a model developed by Quan and Harris for seismic surveying, a signal attenuation coefficient α_0 has been defined, and a statistically based method that estimates the attenuation coefficient from the spectral centroid downshift over a range of frequencies has been performed. The model states that the spectral centroid downshift is proportional to a path integral through the attenuation distribution and can be used as observed data to reconstruct the attenuation distribution tomographically.

The tomographic problem has been implemented in Matlab® software environment. Numerical modelling assumes straight rays from source transducer to receivers, and involves an ill conditioned system of linear equations. The SIRT (Simultaneous Iteration Reconstruction Technique) iterative method has been implemented and applied to solve the system. The solving algorithm has been implemented in an automated procedure that allows the user to easily obtain a map of the attenuation distribution in the tomographic section. The LabView®'s native virtual instruments have been used.

The preliminary results since now achieved showed that the computerised attenuation tomography imaging can successfully apply to the stone masonry, and confirmed the suitability of the proposed approach to non destructive testing of building materials.

Further researches, currently ongoing, are deepening the analysis of the issues which affect the algebraic problem conditioning. Moreover, the current researches are implementing different inversion algorithms, such as ART (Algebraic Reconstruction Technique), SVD (Singular Value Decomposition), SVDT (Truncated SVD), chosen among the most robust and commonly used, for determining the distribution of the attenuation coefficient in the tomographic section, with the aim of highlighting the most suitable techniques for the algebraic problem solution.

References

[1] Fib bulletin 17, "Management, maintenance and strengthening of concrete structures", 2002.

[2] B.D. Boro, H. Reis (Eds.), "NDE of Infrastructure," ASNT Topics on NDE, 2, ASNT,Columbus, 1998.

[3] G. Concu, B. De Nicolo, F. Mistretta, "Comparative evaluation of two non-destructive acoustic techniques applied in limestone masonry diagnosis", Proc. of the 33rd Int. Conf. and Exhib. Defectoscopy 2003, Ostrava, 2003.

[4] G. Concu, B. De Nicolo, F. Mistretta, L. Pani, "Experimental evaluation of Indirect Sonic Wave Transmission Technique in the diagnosis and monitoring of concrete structures and infrastructures", Proc. of the 2nd ICCRRR, Cape Town, 2008.

[5] G. Concu, F. Mistretta "Non-destructive sonic testing of limestone masonry buildings", Proc. of RILEM SACoMaTiS 2008, Varenna, 2008.

[6] Y. Bar-Cohen, R.L. Crane, "Acoustic-backscattering imaging of subcritical flaws in composites", Materials Evaluation, 40, 970-975, 1982.

[7] M. Berra, L. Binda, G. Baronio, A. Faticcioni "Ultrasonic pulse transmission: a proposal to evaluate the efficiency of masonry strengthening by grouting", Proc. of the 2nd Int. Conf. on Non-destructive Testing, Microanaytical Methods and Environment Evaluation for Study and Conservation of Works of Art, Perugia, 1988.

[8] Y. Bar-Cohen, A.K. Mal, C.C. Yin, "Ultrasonic Nondestructive Evaluation of Cracked Composite Laminates", Review of Progress in Quantitative Nondestructive Evaluation, 10(B), 1531-1538, 1991.

[9] S. Abbaneo, L. Binda, M. Berra, A. Faticcioni, "Non-destructive evaluation of brick-masonry structures: calibration of sonic wave propagation procedures", Proc. of the Int. Symp. Non-destructive testing in civil engineering, Berlin, 1995.

[10] M. Berra, L. Binda, L. Anti, A. Fatticcioni, "Utilisation of sonic tests to evaluate damaged and repaired masonries", Proc. of NDT Evaluation of Civil Struct. and Mat., Boulder, 1992.

[11] L. Binda, A. Saisi, C. Tiraboschi, “Application of sonic tests to the diagnosis of damaged and repaired structures”, NDT&E International, 34(2), 123-138, 2001.
[12] L. Ericsson, T. Stepinski, “Algorithms for suppressing ultrasonic backscattering from material structure”, Ultrasonics, 40 (1-8), 733-734, 2002.
[13] A. Shinde, and Z. Hou, “A wavelet packet based shifting process and its application for Structural Health Monitoring”, Structural Health Monitoring, 4, 153, 2005.
[14] W.J. Staszewski, “Structural and mechanical damage detection using wavelets”, The Shock and Vibration Digest, 30, 457-472, 1998.
[15] M.M. Reda Taha, A. Noureldin, J.L. Lucero, T.J. Baca, “Wavelet Transform for Structural Health Monitoring: a compendium of uses and features”, Structural Health Monitoring, 5, 267, 2006.
[16] W.-X. Ren, G. De Roeck, “Structural damage identification using modal data. I: simulation verification”, ASCE Journal of Structural Engineering, 128(1), 87-95, 2002.
[17] D. Akers, C. Vaccaro, S. Ellworth, D. Pettit, “The effect of porosity density and configuration in composite materials on the ultrasonic waveform”, Review of Progress in Quantitative Nondestructive Evaluation, 15, 1239-1246, 1996.
[18] D.V. Perov, A.B. Rinkevich, O.V. Nemytova, “Interaction of pulse ultrasonic signals with reflectors of different types”, Russian Journal of Nondestructive Testing, 43(6), 369-377, 2007.
[19] D.V. Perov, A.B. Rinkevich, “Acoustic pulse signal diffraction from different reflectors in an elastic medium”, Insight, 50(4), 216-217, 2008.
[20] J. Krautkramer, H. Krautkramer, “Ultrasonic testing of materials”, Springer Verlag, New York, 1990.
[21] EN 12504-4, “Testing concrete- Part 4: Determination of ultrasonic pulse velocity”, 2004.
[22] EN 14579, “Natural stone test methods – Determination of sound speed propagation”, 2004.
[23] A.C. Kak, M. Slaney, “Principles of Computerized Tomographic Imaging”, IEEE, Inc., New York: IEEE Press, 1988.
[24] G.T. Herman, “Image Reconstruction from Projections: The fundamentals of Computerized Tomography”, Academic Publishers, New York, 1980.
[25] J.G. Berryman, “Non linear inversion and tomography” Lecture notes, Earth Resource Laboratory, MIT, 1991.
[26] S. Ivansson, “Seismic Borehole Tomography – Theory and Computational Methods”. Proc. IEEE, 74, 328-338, 1986.
[27] Y. Hengyong, J. Patrick La Riviere, X. Tang, “Development of Computed Tomography Algorithms”, International Journal of Biomedical Imaging, 1-3, 2006.
[28] P. Belanger, P. Cawley, “Feasibility of low frequency straight-ray guided wave tomography”, NDT&E International, 42, 113-119, 2009.
[29] J. Rhazi, “Evaluation of concrete structures by the Acoustic Tomography Technique”, Structural Health Monitoring, 5, 333, 2006.

[30] J. Leonard Bond, W.F. Kepler, D.M. Frangopol, "Improved assessment of mass concrete dams using acoustic travel time tomography. Part I: theory", Construction and Building Materials, 14, 133-146, 2000.
[31] W.F. Kepler, J. Leonard Bond, D.M. Frangopol, "Improved assessment of mass concrete dams using acoustic travel time tomography. Part II: application", Construction and Building Materials, 14, 147-156, 2000.
[32] I.L. Meglis, T. Chow, C.D. Martin, R.P. Young, "Assessing in situ microcrack damage using ultrasonic velocity tomography", International Journal of Rock Mechanics & Mining Sciences, 42, 25-34, 2005.
[33] M. Camplani, B. Cannas, S. Carcangiu, G. Concu, A. Fanni, A. Montisci, M.L. Mulas, "Acoustic Tomography for non destructive testing of stone masonry", ICCSA 2008, Part II, LNCS 5073, 596-605, 2008.
[34] B. Cannas, S. Carcangiu, G. Concu, M. Di Mauro, A. Fanni, A. Montisci, M.L. Mulas, "A comparison of tomographic reconstruction algorithms for acoustic non destructive testing of stone masonry", Proc. of the 1st International Symposium on Life-Cycle Civil Engineering, Varenna, 2008.
[35] A.I. Best, C. McCann, J. Sothcott, "The relationships between the velocities, attenuations, and petrophysical properties of reservoir sedimentary rocks", Geophysical Prospection, 42, 151-178, 1994.
[36] J.A. Hudson, "Wave speeds and attenuation of elastic waves in material containing cracks", Geophysical Journal International, 64, 133-50, 1981.
[37] D.H. Johnston, "Attenuation: A state-of-art summary: Seismic Wave Attenuation", in Toksöz and Johnston, Eds., Geophysics reprint series, 2, Soc. of Expl. Geophys., 1981.
[38] Y. Quan, J.M. Harris, "Seismic attenuation tomography using the frequency shift method", Geophysics, 62(3), 895-905, 1997.
[39] P. Gilbert, "Iterative methods for the reconstruction of three-dimensional objects from projections" Journal of Theoretical Biology, 36, 105-117, 1972.
[40] T.W. Lo, P. Inderwiesen, "Fundamentals of Seismic Tomography", Soc. of Expl. Geoph., Tulsa, 1994.
[41] R. Gordon, "A tutorial on ART" IEEE Trans. Nuclear Science, NS-21, 78-93, 1974.
[42] R. Gordon, R. Bender, G.T. Herman, "Algebraic Reconstruction Technique (ART) for three-dimensional electron microscopy and x-ray photography", Journal of Theoretical Biology, 29, 471-81, 1970.
[43] K.A. Dines, R.J. Lytle, "Computerized geophysical tomography", Proc. IEEE 67(7), 1065-1073,1979.
[44] V.A. Lakshiminarayanan, A. Lent, "Methods of least squares and SIRT in reconstruction", Journal of Theoretical Biology, 76, 267-295, 1979.
[45] D.P. Jansen, D.A. Hutchins, P.J. Ungar, R.P. Young, "Acoustic tomography in solids using a bent ray SIRT algorithm", Nondestructive Testing and Evaluation, 6, 131-148, 1991.
[46] Watson, D.F. "Contouring: a guide to the analysis and display of spatial data", Pergamon Press, New York, 1992.
[47] A.R.H. Swan, M. Sandilands, "Introduction to Geological Data Analysis", Oxford: Blackwell Science, Ltd., 1995.

Acknowledgments

Authors gratefully acknowledge the support provided by Regione Sardegna - Sardegna Ricerche - RRI under the grant POR SARDEGNA 2000-2006 MISURA 3.13 - Ricerca e sviluppo tecnologico nelle imprese e territorio.